

# 3D Effects of Surface Construction Over Existing Subway Tunnels

*M. Abdel-Meguid, R. K. Rowe,\* and K. Y. Lo*

---

Graduate student, Department of Civil Engineering,  
University of Western Ontario, London,  
Ontario, N6A 5B9.  
Email: [maabdelm@uwo.ca](mailto:maabdelm@uwo.ca) Fax: (519) 661-3779

Professor, Geo-Engineering Center of Queens-RMC,  
Department of Civil Engineering, Queens University,  
Kingston, Ontario, K7L 3N6  
Email: [kerry@civil.queens.ca](mailto:kerry@civil.queens.ca) Fax: (613) 533-6934

Emeritus professor and director, Geotechnical Research  
Centre, Department of Civil Engineering, University of  
Western Ontario, London, Ontario, N6A 5B9.

---

**ABSTRACT.** A 3D elasto-plastic finite element model is used to examine the effect of construction over two existing tunnels. Tunnel deformation and the change in lining shape are compared with the field measurements of the York-Mills Centre project constructed in 1989 over an existing Toronto subway tunnel. The criterion for potential damage to the tunnel liner is established based on the extreme fiber stresses of the lining. Typical 2D plane strain analyses were also conducted to investigate the importance of the 3D analysis in this case. Reasonable agreement is found between the observed field measurements and the predicted results using the 3D numerical simulation.

## I. INTRODUCTION

The construction of the York-Mills Centre, a multi-story commercial building, required surface excavation above and adjacent to two Toronto Transit Commission (TTC) subway tunnels. While the loads from the super-structures may be transmitted to the firm ground below

---

*Key Words and Phrases.* tunneling, lining, three-dimensional, finite element, excavation, longitudinal stability, modeling.

---

\* Corresponding author. E-mail: [kerry@civil.queens.ca](mailto:kerry@civil.queens.ca) Fax: (613) 533-6934

the tunnel using girders and caissons to span the tunnel, the effects of lining deformations and stresses due to the excavation for the substructure cannot be so readily avoided. The clearance between the base of the excavation and the subway lining was small enough to raise concern regarding the influence of the new construction on the structural integrity of the subway tunnel liner.

As part of the evaluation process, Lo and Ramsay [1] presented a method of analysis to predict the displacements of the tunnel lining using 2D plane strain analysis for both the transverse and longitudinal cross-sections of the tunnel. The construction of the existing tunnel, however, was not simulated in this analysis. A 3D finite layer analysis was also conducted to predict the ground heave along the longitudinal direction of the tunnel neglecting the effect of the existing tunnels. A monitoring program was developed to record the movement of the lining at selected rings along the tunnel during construction. Based on the results of the two analyses, they concluded that displacements of the tunnel lining might be conservatively predicted. However, the analysis did not predict the ultimate stress-state in the lining because it will depend on the existing stresses which, in turn, will depend on the past construction history of the tunnels. Rather, the initial stresses in the lining were assumed to be approximately hydrostatic.

Current design procedures do not typically model the detailed 3D aspects of construction over subway tunnels, which usually involves unsymmetrical and highly skewed geometry. The objective of this article is to describe a 3D model suitable for analyzing construction of an existing tunnel, the lining activation, and subsequent surface construction over the tunnel in a single numerical model and to show how this model was used to study the case of York-Mills Centre. Particular emphasis is placed on the prediction of tunnel displacement, the change in lining shape, and the factor of safety for the structural elements during excavation.

## II. METHOD OF ANALYSIS

The analyses are performed using a 3D elasto-plastic finite element computer program developed based on the library of routines published by Smith and Griffiths [2] employing the aspects presented below.

### A. Full 3D Analysis

Solution accuracy depends primarily on how well the assumed variation of stress within an element fits the actual variation in a structure. Linear 3D elements such as the 8-noded brick element are quite stiff in certain deformation modes and often provide inaccurate results, especially for bending type problems. Lee and Rowe [3] examined the use of 11/8 nonconforming elements for studying the 3D ground deformations due to tunneling in soft ground. They found that while these elements provided considerably improved performance relative to the 8-noded elements and were suitable for analysis where there was only a limited amount of plasticity, the 11/8 nonconforming elements were not suitable for use in predicting collapse loads under constant volume conditions.

In the present study, 20-noded brick elements are used to model the ground continuum and the tunnel liner. The use of thin continuum elements to model the tunnel liner has proved to perform well when compared with a specially formulated shell elements (Augarde and Burd [4]). The performance of the 20-noded element has been checked against simple cases where closed-form solutions exist for comparison, including problems of beam bending, open excavations, and

underground tunnels. Details of the problems and solutions are given elsewhere (Abdel-Meguid [5]).

## B. Varied Construction Sequences

Material is removed at several stages so that, for the nonlinear analyses, the final stress data is appropriate to the sequence of excavation that would be performed. This process must be conducted in such a way that equilibrium is maintained in the soil elements around the tunnel. Element removal was carried out using procedure described by Brown and Booker [6]. Initially, the ground is stressed by its own weight. For each excavation stage, the geometry is modified and a new stiffness matrix and load vector are formed. The loads are removed in increments and the nonlinear equations solved using a modified Newton-Raphson technique. A full integration scheme (27 integration points) was used in the present analysis.

## C. Material Nonlinearity

The commonly used Mohr-Coulomb failure criterion is adopted in the present analysis. This failure criterion has an irregular hexagonal shape in principal stress space as shown in Figure 1a. The function may be expressed as

$$F = \sigma_m \sin \phi + \bar{\sigma} \left( \frac{\cos \theta}{\sqrt{3}} - \frac{\sin \theta \sin \phi}{3} \right) - c \cos \phi \quad (1)$$

where,

$$\sigma_m = s/\sqrt{3} \quad (2a)$$

$$\bar{\sigma} = t\sqrt{(3/2)} \quad (2b)$$

$$s = \frac{1}{\sqrt{3}} (\sigma_x + \sigma_y + \sigma_z) \quad (2c)$$

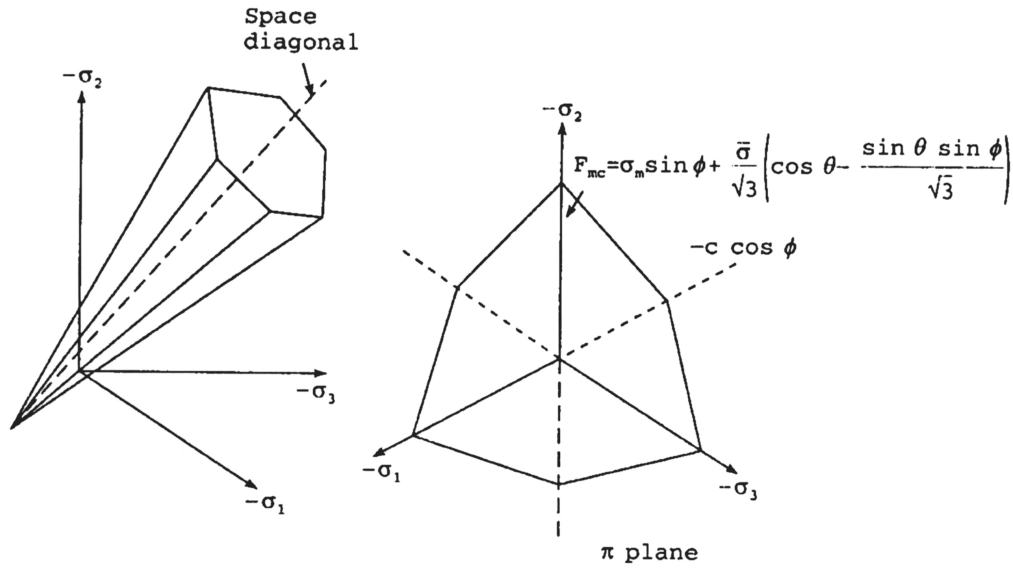
$$t = \frac{1}{\sqrt{3}} \left[ (\sigma_x - \sigma_y)^2 + (\sigma_y - \sigma_z)^2 + (\sigma_z - \sigma_x)^2 + 6\tau_{xy}^2 + 6\tau_{yz}^2 + 6\tau_{zx}^2 \right]^{1/2} \quad (2d)$$

$$\theta = \frac{1}{3} \arcsin \left( \frac{-3\sqrt{6}J}{t^3} \right) \quad (2e)$$

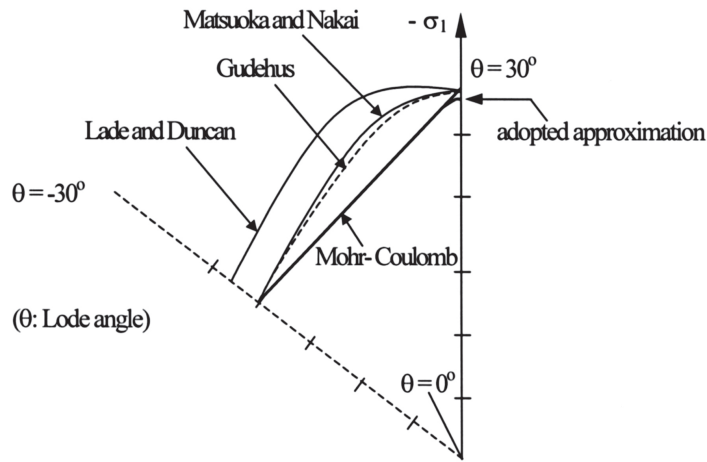
$$J = s_x s_y s_z - s_x \tau_{yz}^2 - s_y \tau_{zx}^2 - s_z \tau_{xy}^2 + 2\tau_{xy} \tau_{yz} \tau_{zx} \quad (2f)$$

and

$$s_x = (2\sigma_x - \sigma_y - \sigma_z)/3, \text{ etc.} \quad (2g)$$



a) Mohr-Coulomb surface



b) Some smooth approximations in the  $\pi$ -plane

FIGURE 1. Mohr Coulomb failure criterion.

For a noncontinuous surface, the derivative of the function  $F$  becomes indeterminate. In the case of Mohr-Coulomb surface, this occurs when the angular invariant  $\theta = \pm 30^\circ$ . To overcome this problem several smoothing functions or alternative constitutive models have been proposed such as those by Gudehus [7], Matsuoka and Nakai [8] and Lade and Duncan [9] as shown in Figure 1b.

These surfaces lie outside the Mohr-Coulomb surface and even though they have certain advantages in computational work, the implied friction angle differs by several degrees when fitted to Mohr-Coulomb surface for certain stress paths as indicated by Griffiths [10] and Zienkiewicz and Pande [11].

In the present study, the smoothing algorithm of Smith and Griffiths [2] is adopted, where the hexagonal surface is replaced by a smooth conical surface only if

$$|\sin \theta| > 0.49$$

The conical surfaces are those obtained by substituting either  $\theta = 30^\circ$  or  $\theta = -30^\circ$  into equation (1), depending upon the sign of  $\theta$  as it approaches  $\pm 30^\circ$ . The effect of this smoothing is small as shown in Figure 1b.

It has been reported (Addenbrooke et al. [12]) that nonlinear pre-failure deformation models are necessary to achieve the correct surface settlement in London clay. This is true for soils exhibiting nonlinear behavior at small strain. In this particular case the need to model small strain nonlinearity is finessed by using a modulus profile deduced from field observations (as discussed later) and hence the small strain effect is incorporated in the modulus profile.

#### D. Solution Algorithm

In a 3D analysis that does not seek to model collapse, reforming and factorizing the global stiffness matrix for the tangent stiffness approach is computationally very costly. Thus for the analyses reported herein, a simple viscoplastic algorithm (Zienkiewicz and Corneau [13]) with a modified Newton-Raphson iterative scheme is used to redistribute stresses that have strayed outside the failure surface.

#### E. Pre and Post Processing

The graphical interface program GID [14] was used to generate the finite element mesh and to interpret the results of the 2D and 3D analyses.

### III. PROJECT DESCRIPTION AND SITE CONDITIONS

Phase III of the York Mills Centre, located at the northeast corner of the intersection of Yonge Street and York Mills Road in Toronto, Ontario, Canada was constructed over two Toronto Transit subway tunnels. To reduce the net structural loading onto the tunnels, the loads from the building were transferred to the subsoil below the invert of the tunnels using large diameter (1.1 m to 2.4 m) caissons that span the tunnel. The excavation for the substructure was approximately 100 m by 70 m, with area of about 90 m by 40 m directly over the tunnels, as shown in Figure 2. The depth of the excavation is generally 7 to 9 m deep. The clearance distance between the excavation base and the crown of tunnels was about 2 m at the closest locations.

The subway tunnels at York-Mills were constructed in the late 1960s. The lining is composed of cast-iron rings of 4.9 m internal diameter. Each 0.61 m ring is made up of eight segments

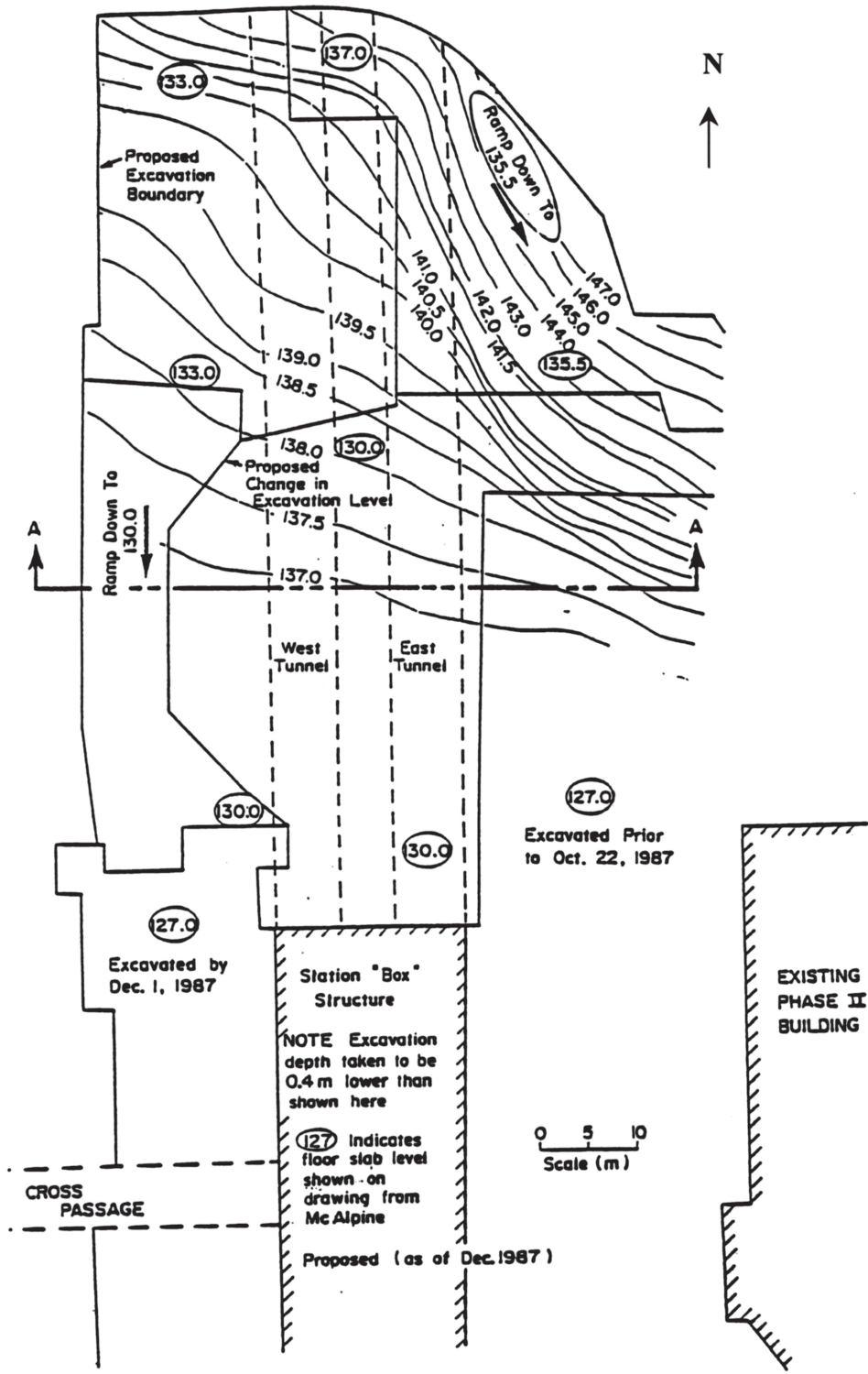


FIGURE 2. Project layout showing the excavation levels. (Adapted from Lo and Ramsay [1].)

connected by three 2.54 cm diameter bolts with a crown key. In the axial direction, the segments are connected by four 4.13 cm diameter bolts with a total of 32 bolts joining the adjacent rings together. Two grout holes were provided in each segment.

Part of the subway tunnels in the York-Mills project area was shield-driven under compressed air. The joints in the adjacent rings were staggered. Other parts of the tunnel were constructed by hand after dewatering, and radial joints in the adjacent rings were not staggered. No difficulty was reported during the tunnel construction.

The subsoil conditions involve a relatively uniform deposit of gray dense silt, approximately 47 m thick, overlying bedrock. The water content was 11.4% and the unit weight was 22.6% kN/m<sup>3</sup>. The modulus profiles were obtained based on tests conducted on block samples recovered from a test trench at an excavation east of the subway station at El. 126 m. Anisotropic consolidated drained tests were performed on the samples in both compression and extension modes. In this class of problem, the extension modulus of deformation at small strains plays an important role in the analysis (Ng and Lo [15]). Results of the triaxial extension tests showed that the strain at failure was approximately 1% with a small dilation during shear. Poisson's ratio was found to be 0.42. The effective friction angle,  $\phi'$ , for both compression and extension tests was about 40° and the soil cohesion was close to zero.

A Young's modulus profile (see Figure 3) was obtained based on data from monitoring the heave of the excavation that was proceeding directly west of the subway station. Magnetic extensometers were installed at two points and the heave at six different depths was measured as local excavation was carried out in this area. A 3D finite layer analysis program, FLANS (Rowe and Booker [16]) was then used to back calculate the extension Young's modulus profile. Details of the field results have been reported by Lo and Ramsay [1].

#### IV. ANALYSIS DETAILS

A parametric study was conducted to check that the finite element mesh, boundary locations, and other numerical parameters such as load increment size were adequate. The lateral boundaries of the mesh were located such that they would not significantly influence the predicted displacements of the tunnel lining. To meet this criterion it was necessary to locate the boundaries 90 m from the tunnel centerlines in the x-direction and 100 m from the excavation walls in y-direction (see Figure 4). The load was removed in ten increments for each of the four excavation stages. Convergence was considered to have occurred when the stresses at all gauss points satisfied the failure criterion and global equilibrium to within a tolerance of 0.1%.

##### A. Modeling Considerations

Some approximations in the excavation geometry were necessary to simplify the mesh generation process and to reduce the mesh size. In this context, a rectangular excavation shape is assumed with a depth from the ground surface ranging from 12 to 2 m deep close to the subway station. Full contact between the existing tunnel lining and the surrounding ground is assumed.

The 3D finite element analysis was performed using 1470 20-noded isoparametric elements with a total of 7098 nodes arranged as shown in Figure 4. Because of the unsymmetrical nature of the excavation it was necessary to model both tunnels as well as the till to a considerable

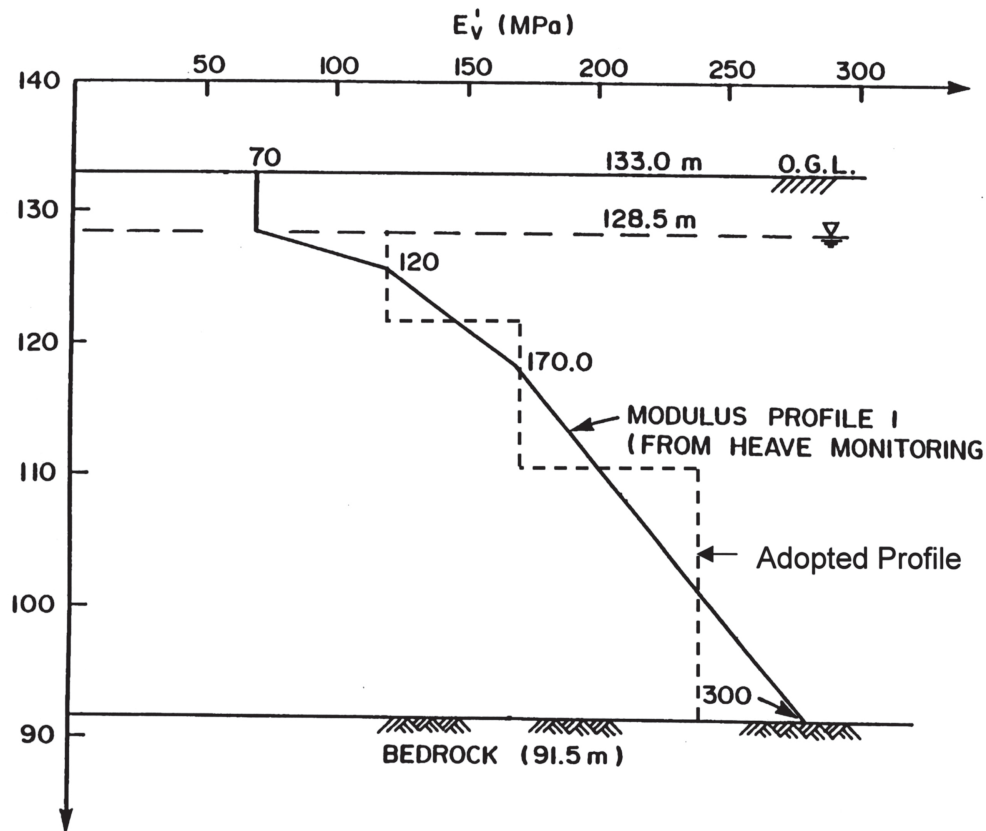


FIGURE 3. Distribution of unloading modulus with depth. (Adapted from Lo and Ramsay [1].)

distance on either side of the tunnels. Nodes along the vertical boundaries may translate freely along the boundaries but are fixed against displacements normal to these boundaries. The nodes at the base are fixed against displacements in both directions.

It is known that segmented cast iron linings are not monolithic and, in fact, are more flexible than the uniform cross section of continuous liner because the stiffness at the joints may be appreciably less than elsewhere. This phenomenon can be taken into account either by modeling contact joints directly or by using an equivalent ring with a smaller inertia (Muir Wood [17]). In this study, the segmented cast iron lining of the subway tunnels are modeled as prismatic 20-noded solid elements with a finite width and modulus ( $EA$ ) equivalent to that of the real lining. The segmental nature of the lining was considered by reducing the Young's modulus of the liner elements. Although higher lining flexibility in the longitudinal direction is expected, a compromise reduction value of 25% was adopted.

To simulate the effect of the existing subway station box and the supporting walls at the excavation boundary, the material properties of the elements at this side of excavation were replaced by the elements properties of the subway station at the third step of analysis. The numerical input parameters for the soil and the tunnel lining are listed in Table 1.

To evaluate the effects of construction on the tunnels, it is important to assess the current state of stress in the lining so that incremental changes due to construction would not lead to



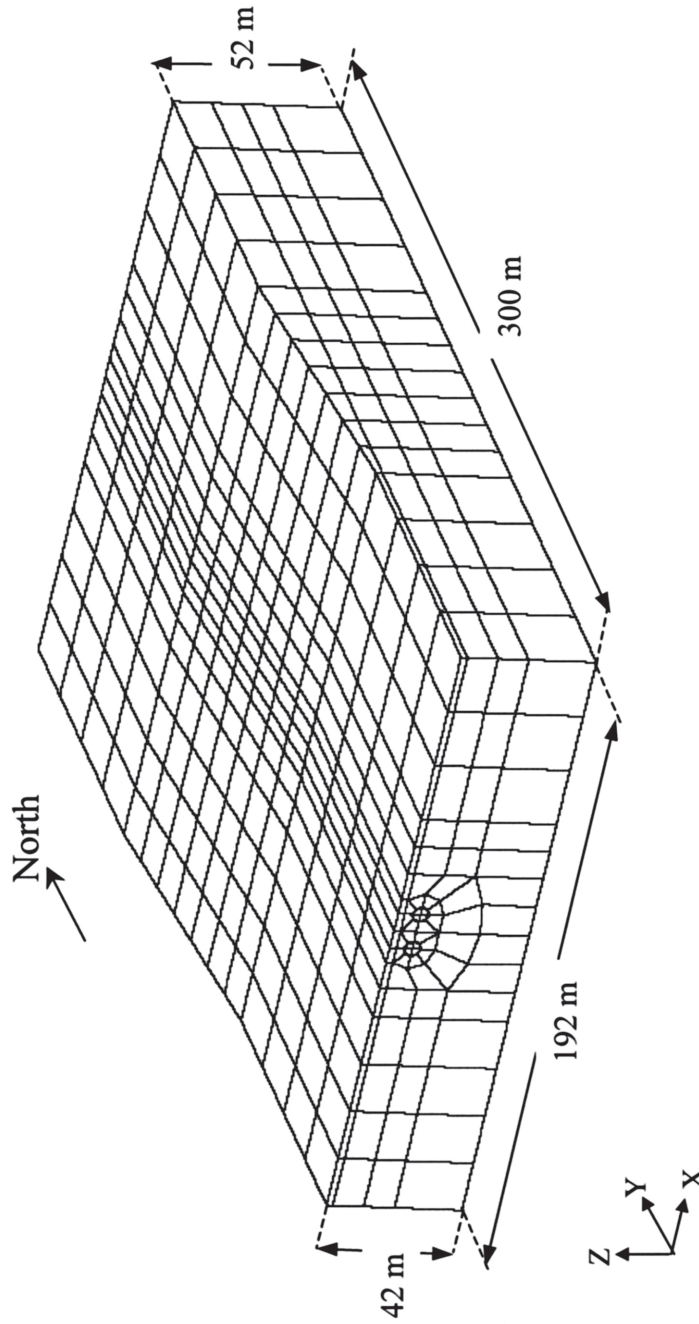


FIGURE 4. Finite element mesh used in the 3D analysis.

**TABLE 1**  
**Input Parameters Used in the 3D Analysis**

<b>Till Properties</b>	
Unit weight ( $\gamma$ )	22.5 kN/m <sup>3</sup>
Coefficient of earth pressure ( $K_0$ )	0.67
Elastic modulus profile (E)	Adopted profile in Figure 3
Poisson's ratio ( $\nu$ )	0.4
Cohesion intercept ( $c'$ )	0.2 kN/m <sup>2</sup>
Effective friction angle ( $\phi'$ )	40°
Angle of dilatancy ( $\varphi$ )	0
<b>Tunnel Lining Properties</b>	
Elastic modulus	$1 \times 10^8$ kN/m <sup>2</sup>
Equivalent (EA)	$3.4 \times 10^7$ kN/m
Poisson's ratio ( $\nu$ )	0.25
Compressive strength	900 MPa
Bolts tensile yield stress	230 MPa
Bolts allowable shear stresses	70 MPa
<b>Subway Station Box</b>	
Elastic modulus	$1 \times 10^9$ kN/m <sup>2</sup>
Poisson's ratio ( $\nu$ )	0.2
Compressive strength	900 MPa

stresses exceeding the allowable limits. Several methods of simulating tunnel construction are available such as the 'gap parameter' method (Rowe et al. [18]), the 'convergence-confinement' method (Panet and Guenot [19]), and others. These methods provide a useful tool for predicting the surface settlement due to tunnel construction. Since the present study deals with an existing tunnel, simulation of the detailed tunnel construction process and the corresponding deformations is not of interest. Rather, interest here is to obtain a conservative estimate of the initial stresses in the existing tunnel lining as a starting point for the examination of the effect of surface excavation. Therefore, an alternative, simpler, approximate approach to establishing these stresses was sought.

For the purpose of this study, the construction of the existing tunnels was simulated by instantaneously deactivating the soil elements inside the tunnel and activating the liner. This means that, in this simulation, no ground displacements into the tunnel are allowed to take place before the ground and the lining come into contact. In actual tunnel construction, some radial ground displacements into the tunnel will generally take place at the heading before the final lining is installed and becomes effective in carrying load and resisting further ground displacement. It has been shown (Ghaboussi et al. [20]) that for similar situations the liner stresses generally decrease when radial displacements at the heading are allowed to take place prior to

the ground and liner coming into contact. It can, therefore, be concluded that the computed initial subway lining stresses are on the conservative side.

The supporting caissons were installed after the surface excavation phase was completed. Therefore, their effect on the tunnel lining was not considered in the present study which is only concerned with the conditions due to the excavation.

## B. Simulation of Construction Process

Initially, the finite element mesh was subjected to gravity forces giving rise to the *in situ* stress conditions prior to the original tunnel construction. In the subsequent steps, the construction of the existing tunnels and the surface construction were simulated to coincide with the actual construction procedure as closely as possible by activating and deactivating various elements.

- Step 1: North subway tunnel construction was simulated by deactivating the soil elements within the tunnel and activating the tunnel liner elements.
- Step 2: South subway tunnel construction was simulated, similarly.
- Step 3: The material properties of the original soil elements around the excavation were, then, changed to account for the shoring installation and the stiffness of the subway station.
- Step 4: The surface construction was simulated in two stages according to the construction history of the excavation as shown in Figures 5 and 6, respectively, and the resulting changes in the lining shape and stresses were predicted.

## V. RESULTS OF THE 3D ANALYSIS

### A. Initial Stresses in Subway Linings

In the first two steps of the analysis, the actual sequence of construction of the subway tunnels is simulated. The circumferential thrust,  $N$ , in the lining after the construction of both subway tunnels is presented in nondimensional form, and normalized in terms of the unit weight of the ground,  $\gamma$ , and the depth to the center line of the tunnel,  $H$ , as shown in Figure 7. It was observed that the stresses and deformations of both tunnels are quite symmetrical. This can be attributed to the fact that the distance between the two tubes is greater than the tunnel diameter (about 1.5  $D$ ). However, this stress distribution varied as one moved along the lining axis with increasing the overburden pressure over the lining. The maximum circumferential thrust at the spring-line is about 480 kN/m, which corresponds to a ratio ( $N/\gamma HR$ ) of about 0.7, and at the crown and invert is about 330 kN/m.

### B. Stress and Deformation Changes Resulting from the Surface Excavation

In the fourth step of the analysis, the deformation and stress changes resulting from the surface excavation were estimated. The calculated deformed shape of the lining after the surface construction is shown in Figure 8.

The maximum accumulated vertical movement of the tunnel invert after the final construction stage is 21 mm at a distance of about 70 m from the subway station box. The increase in the

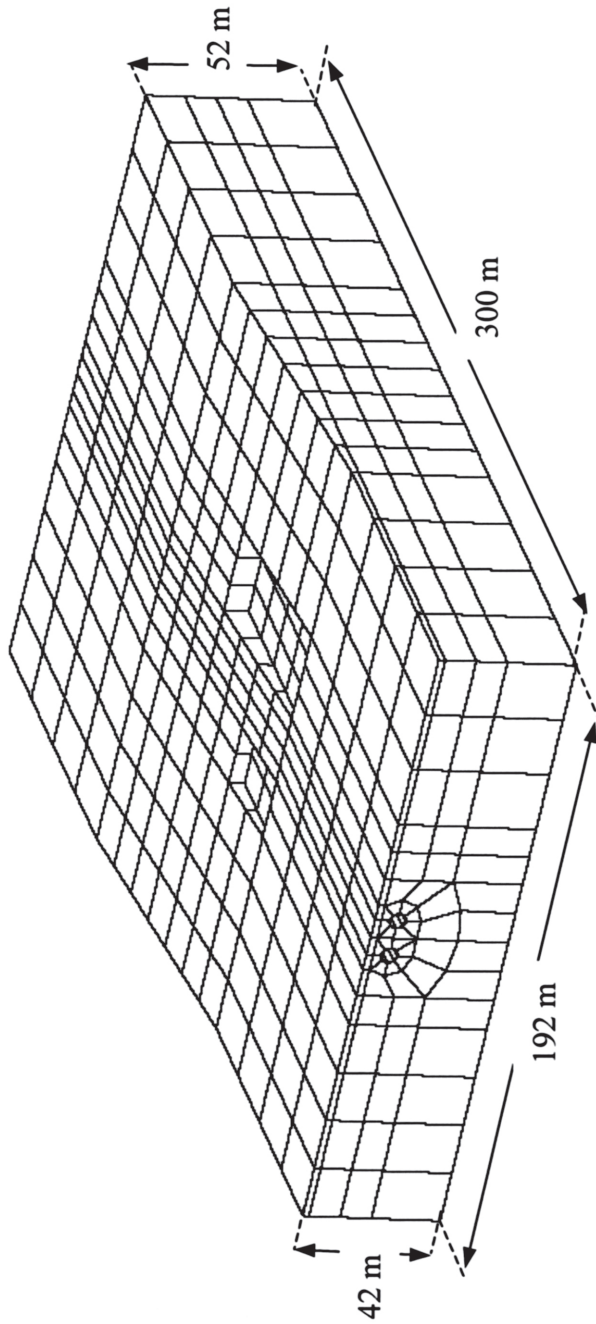


FIGURE 5. First stage of surface excavation.

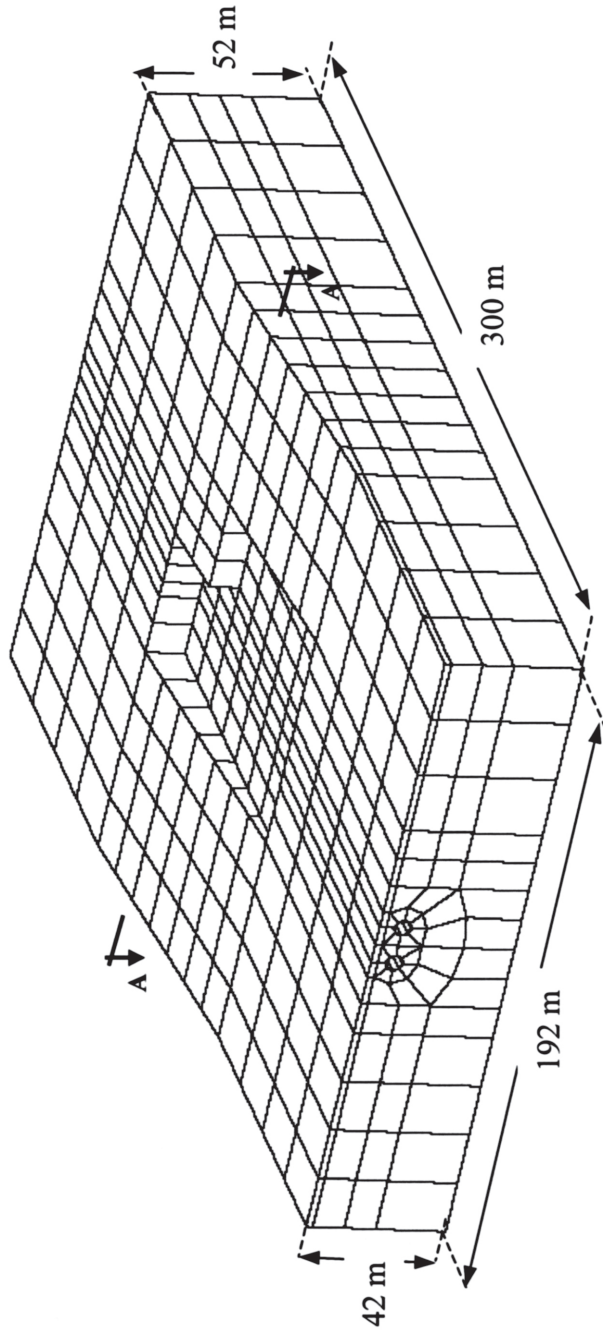


FIGURE 6. Final stage of surface excavation.

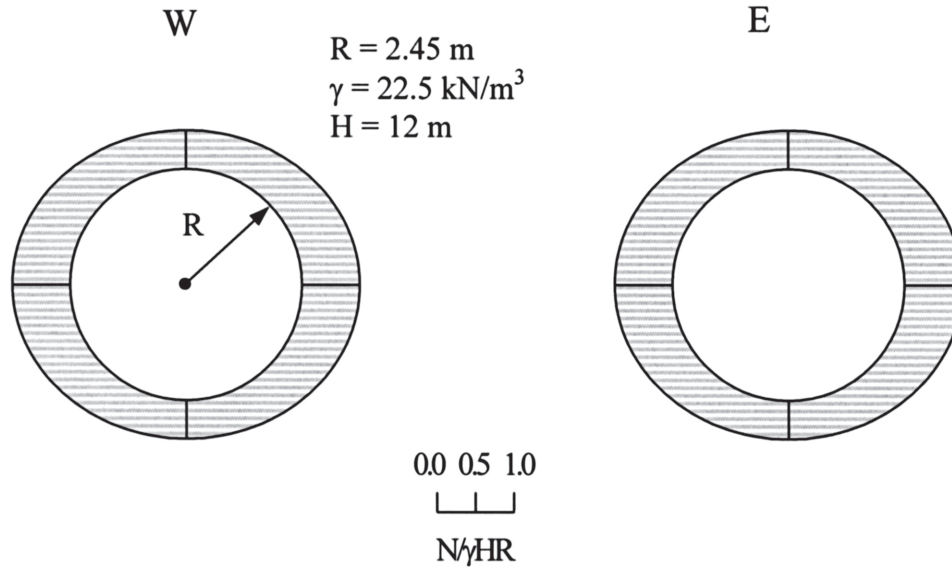


FIGURE 7. Initial thrust of the tunnel linings.

vertical distance between the crown and invert is about 6 mm and the spring-line closure is about 5 mm.

The lining stresses in the longitudinal direction are directly predicted from the results of the 3D analysis. A maximum compressive stress of about 2800 kPa at the extreme bottom fibers of the lining was found to occur in northbound tunnel, at the location of maximum displacement, at distance of 70 m from the subway station. On the other hand, a maximum tensile stress of about 730 kPa at the extreme top fibers of the lining occurred at the location of maximum displacement as shown in Figure 9.

### C. Criterion for Potential Damage to the Liners

The criterion for potential damage to the tunnel liner is established based on the maximum tensile stresses in the extreme fiber of the lining such that the flanges of the two adjacent segments would separate when the tensile stresses exceed the bolt pretension. Another failure mode that may be encountered is the bolt shear failure. The bolts would fail in shear if the shear stresses acting on the bolts were greater than its shear capacity.

For the purpose of calculating the stress levels in the longitudinal bolts, the lining was treated as a “composite section” with only the bolts resisting tension at all locations above the neutral axis, and the skin of the lining carrying compression below the neutral axis as shown in Figure 9.

Based on this approach, the maximum tensile stresses computed in the bolts were in the range of 50 to 70 MPa/bolt at the location of the maximum displacement. This is well below the yield stress (230 MPa) of the bolts. These stresses also suggest that the longitudinal bolts along the tunnel lining retained their pretension (estimated to be 20 to 25% of the tensile strength, i.e.,

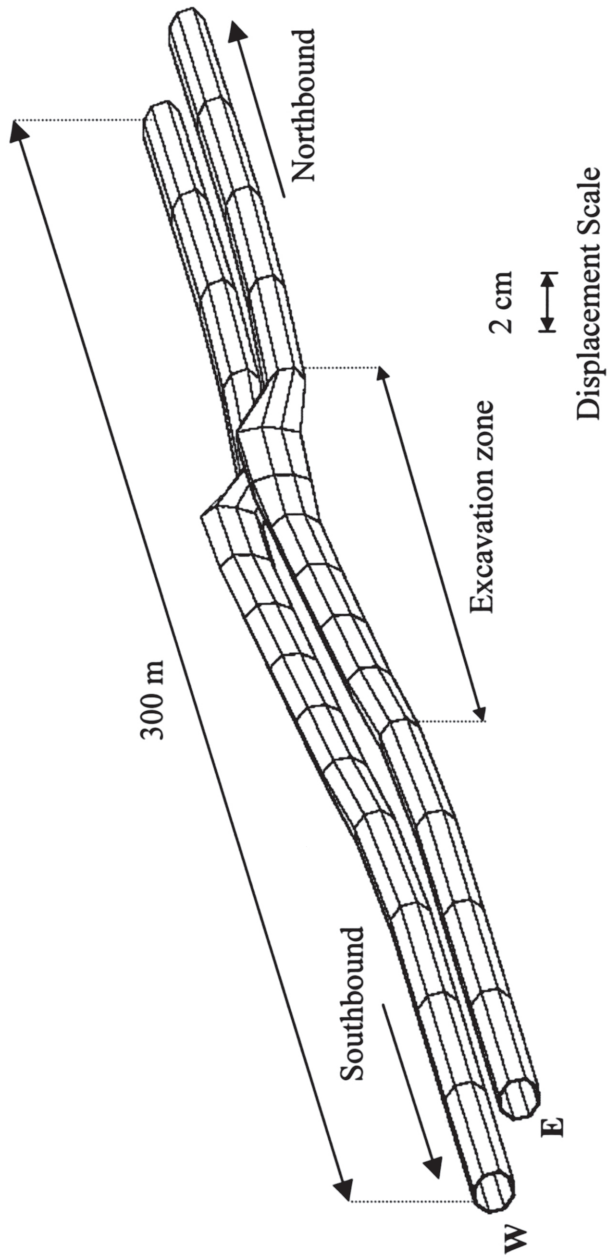


FIGURE 8. Final deformed shape of the lining.

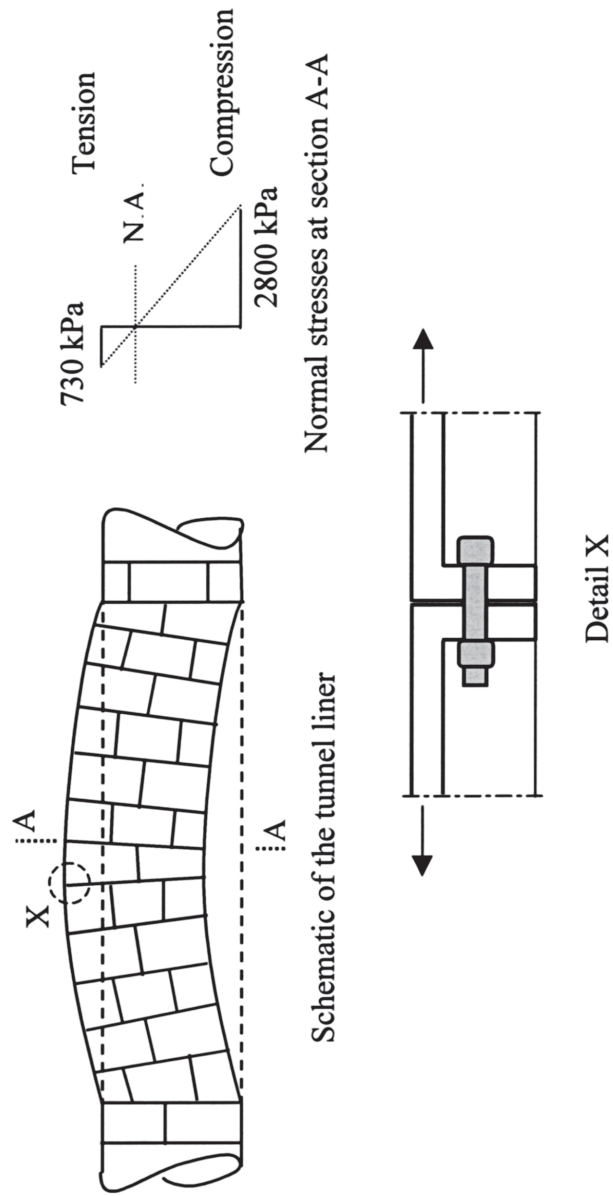


FIGURE 9. Normal stress distribution at the critical cross-section.



45 to 60 MPa) except at the location of high deformation where the stresses were sufficient to increase the tensile stress of the bolts beyond the pretension value causing some separation of the segments flanges. The validity of this prediction was evident from the reported water leak through the tunnel joints close to the location of maximum vertical displacement, at a distance of 65 m from the subway station, during construction. Yielding of the bolts could be reached following flange separation under higher bending moments; however, this was not predicted in either tunnel and was not observed in the field.

## VI. RESULTS OF THE 2D ANALYSIS

In order to investigate the importance of the 3D analysis in this case, a typical two-dimensional (2D) plane strain analysis was performed on one transverse cross-section located at section (A-A) shown in Figure 6. The elements considered in the 2D analysis are 364 8-noded isoparametric elements with a total of 1161 nodes arranged as shown in Figure 10. Nodes along the vertical boundaries may translate freely along the boundaries but are fixed against displacements normal to these boundaries. The nodes at the base are fixed against displacements in both directions. The segmented cast iron lining of the subway tunnels are modeled as prismatic 8-noded solid elements with a finite width and modulus ( $EA$ ) equivalent to that of the real lining. To allow a direct comparison, the numerical details for the 2D analysis were the same as for the 3D analysis (see Figure 11).

Based on the 2D results, the maximum estimated crown heave is about 42 mm. The increase in the vertical distance between the crown and the invert is about 7 mm and the decrease in the horizontal distance between points on the spring-line is about 10 mm.

## VII. COMPARISON OF RESULTS

The deformed shapes of the tunnel lining based on different analyses are shown in Figure 12. This figure also summarizes the results of the maximum vertical displacements calculated from the 2D and 3D analyses. The results of the 3D analysis are shown at a cross-section (A-A) of the tunnel (see Figure 6).

The deformations of the tunnels and lining distortion calculated from the 2D and 3D analyses are summarized in Table 2 along with the field measurements for comparison purpose.

The 2D analysis of the transverse cross-section excessively overpredicted the tunnel heave and, consequently, the lining stresses. The prediction of the stresses in the longitudinal direction, which is of great importance in this problem, may also be approached using the 2D analysis; however, it would require the analysis of longitudinal cross-sections along the tunnels. This problem is not, in fact, a plane strain one and may require other assumptions to obtain an equivalent lining stiffness in the longitudinal direction.

On the other hand, the 3D analysis provided reasonable estimates for the displacements and stresses of the tunnel lining in both the transverse and longitudinal directions. The agreement between predicted values from the 3D analysis and those measured in the field is satisfactory.

The displacement profile predicted using the 3D analysis is plotted against distance from the TTC station in Figure 13 for the northbound tunnel. On the same figure, the measured crown

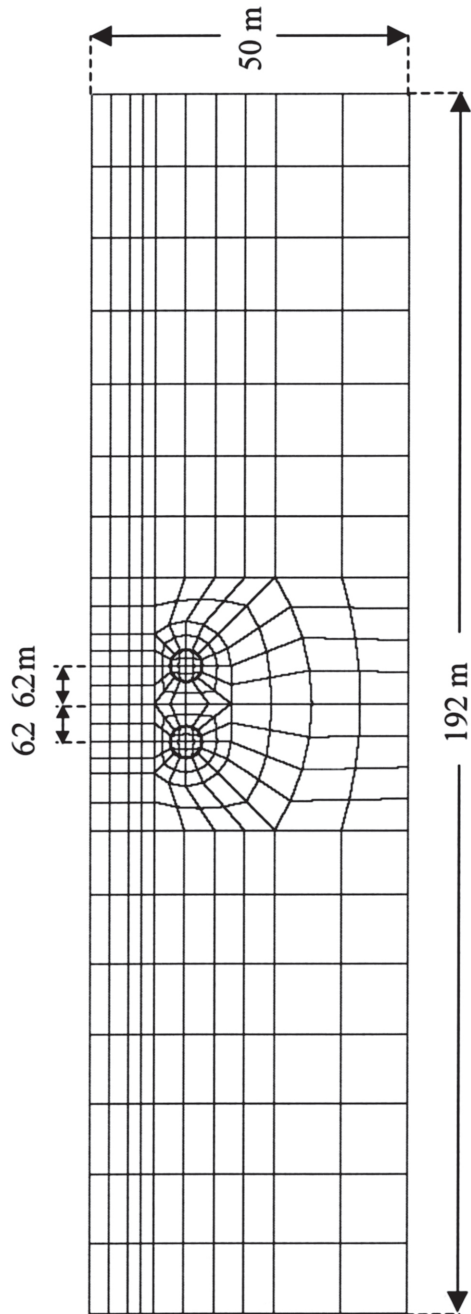
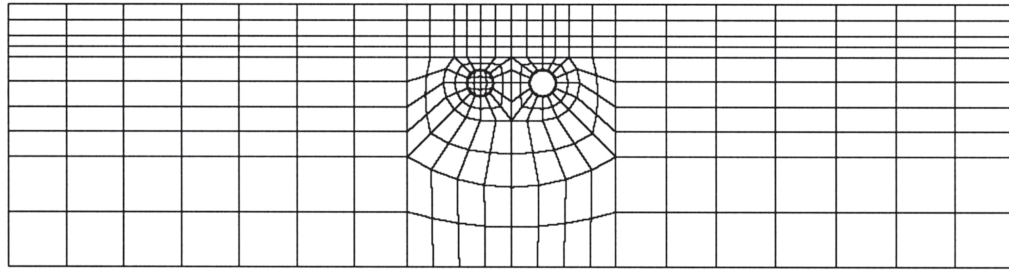
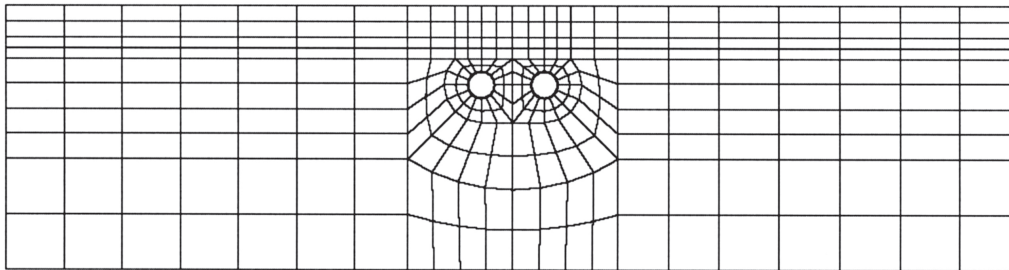


FIGURE 10. Finite element mesh used for the 2D analysis.

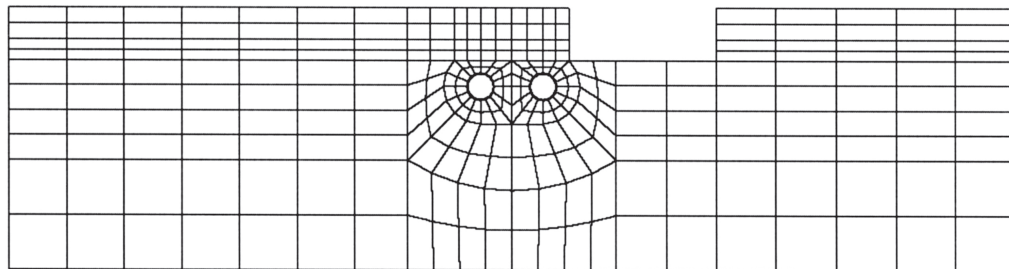
W E



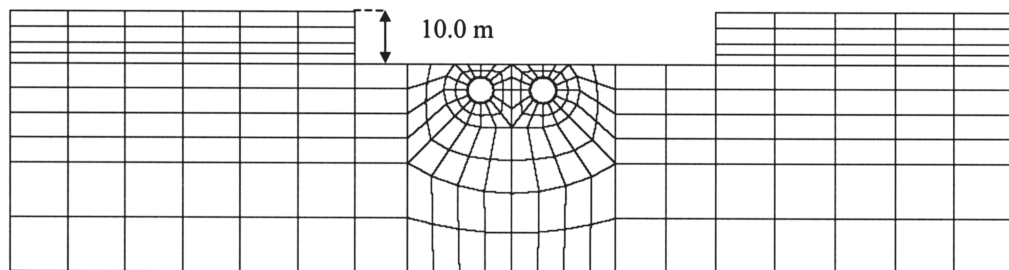
a) Construction of north subway tunnel



b) Construction of south subway tunnel



c) First stage of surface excavation



d) Second stage of surface excavation

FIGURE 11. Simulation of different construction process in 2D analysis.

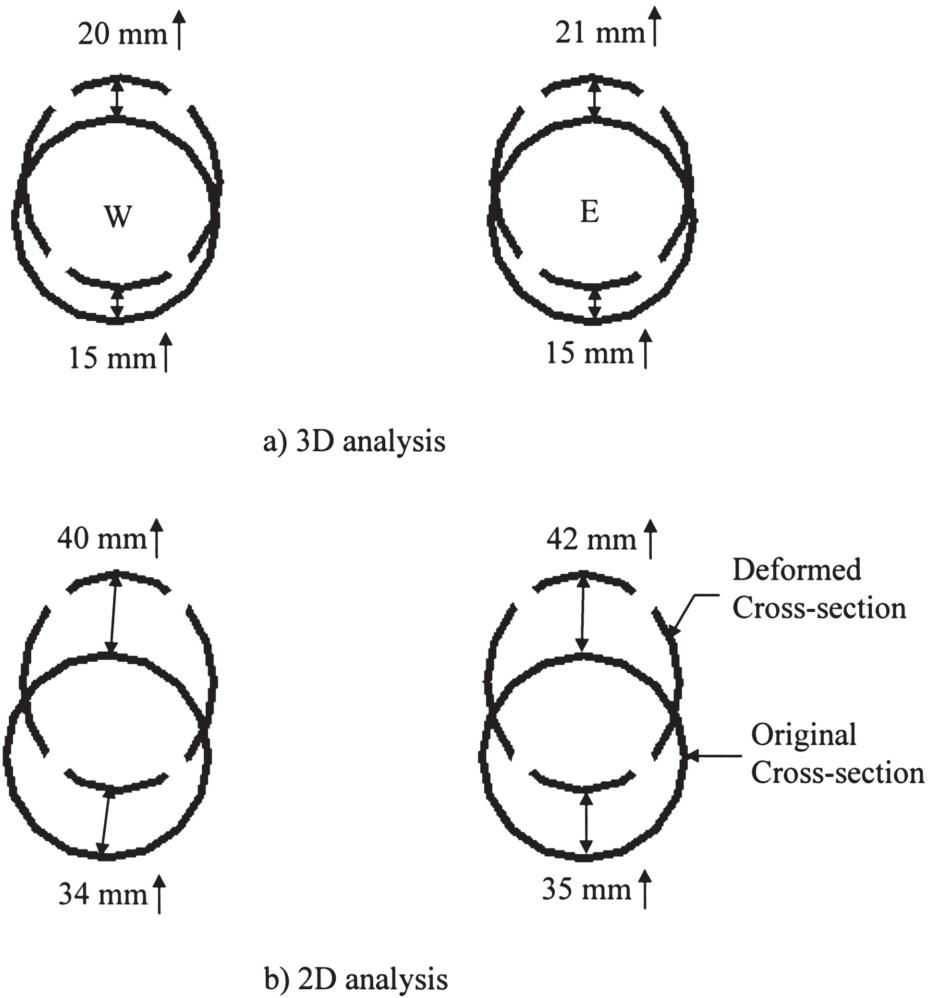


FIGURE 12. Deformed shapes of the lining calculated from different analyses.

heaves at the monitored rings on completion of the general excavation (except the north end) are also plotted. It may be seen that the maximum heave measured was close to but slightly below the maximum heave predicted. It is concluded that the 3D finite element analysis predicted a satisfactory displacement profile as well as stress distribution along the tunnel.

## VIII. COMPUTING RESOURCES

All the mesh-development, 2D analysis, simple 3D analysis runs, and post-processing were performed on PC (750 MHz with 256 Mb memory). The runs for full analysis were performed on IBM Workstation 44P model 270, two-way CPU with 275 MH and 1 Gb memory. With this machine, a typical run time for 3D analysis of the case history took about 6 hours.

**TABLE 2**  
**Comparison of Predicted and Measured Maximum Deformations**

Point of interest	2D analysis*		3D analysis*		Measured	
	South-bound	North-bound	South-bound	North-bound	South-bound	North-bound
Maximum heave (mm)	38	39	17	18	15	17
Crown-invert Extension (mm)	6	7	5	6	4	4
Spring-line Closure (mm)	9	10	4	5	3.5	4.4

\* Deformation resulting from tunnel construction is subtracted for comparison purpose.

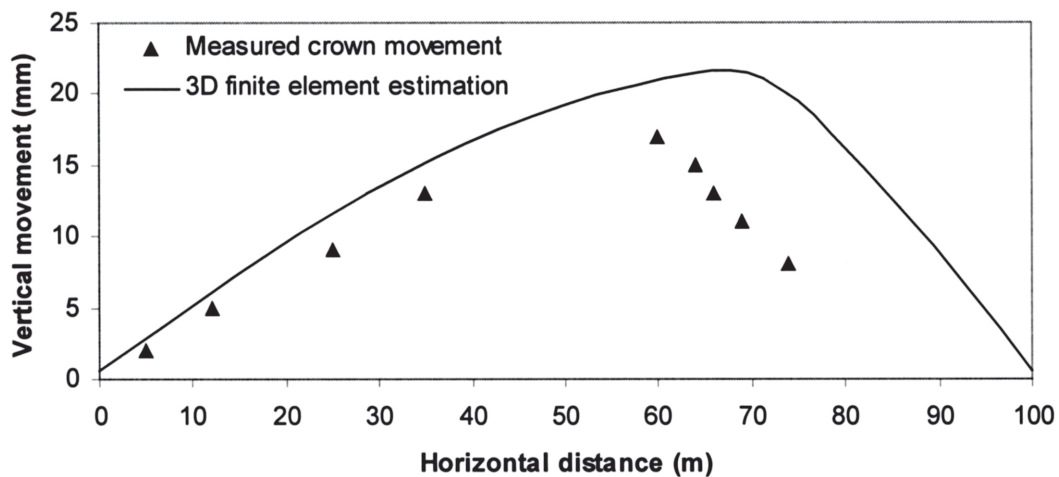


FIGURE 13. Displacement profile along the northbound tunnel.

## IX. SUMMARY AND CONCLUSIONS

Three-dimensional elasto-plastic finite element method was used to simulate the construction of an existing part of Toronto subway tunnels and the response of the lining to the construction of Phase III of York-Mills Centre over the tunnels. The analysis allowed the calculation of the tunnels deformation, the lining distortion, and stresses in both transverse and longitudinal directions. Reasonable agreement is found between the observed field measurements and the predicted results using the proposed numerical simulation.

Current assessment methods are generally based on the two-dimensional finite element analysis; for the cases where the problem geometry is clearly three-dimensional they are likely

to be excessively conservative. For both 2D and 3D analyses, estimating the initial compressive stresses in the tunnel lining before the surface construction is important to the examination of the ultimate state of stresses in the lining and consequently the final displacements in the lining.

A thin layer of 20-noded continuum elements with axial rigidity (EA) equivalent to that of the lining was successfully used to model the segmented cast iron tunnel lining and provided a reasonable estimate for the stresses and deformations based on the 3D finite element analysis.

Reducing the inertia of the lining may be used as a simple numerical tool to account for the fact that the segmented cast iron lining is more flexible than the uniform continuous cross-section. The reduction ratio depends on the number of segments and the stiffness of the joints, and Muir Wood approximate formula appears to be suitable for that purpose in this case.

Excavation over the tunnel forced the lining to behave in the longitudinal direction as a beam-bending problem producing tensile stresses in the top fibers of the lining and compressive stresses in the lower fibers. If the tensile stresses were greater than the initial compressive stresses in the lining, a net tensile stress in the longitudinal bolts is expected. Criteria for potential damage to the lining based on the extreme stresses in the longitudinal direction were established. Joints may separate if the tensile stresses in the lining exceeded the bolt pretension or fail if the yield stresses is exceeded. This criterion should be set depending on the operational criterion for the tunnel and the allowable relative displacements between the lining rings.

Lateral restraint provided by the excavation supporting system and the nearby subway station acts to reduce the extent of heave deformation in the tunnel lining and, thus, the tensile stresses in the longitudinal direction.

## ACKNOWLEDGMENTS

This research is supported by the Natural Sciences and Engineering Research Council of Canada (NSERC). Support in the form of NSERC Post Graduate Scholarship (PGSB) and Ontario Government Scholarship in Science and Technology (OGSST) are also acknowledged.

## REFERENCES

- [1] **K.Y. Lo and J.A. Ramsay**, The effect of construction on existing subway tunnels—a case study from Toronto, *Tunneling and Underground Space Technology*, **6**(109), 287–297, 1990.
- [2] **I.M. Smith and D.V. Griffiths**, *Programming the Finite Element Method*, Third edition, John Wiley, London, 1998.
- [3] **K.M. Lee and R.K. Rowe**, Finite element modeling of the three-dimensional ground deformations due to tunneling in soft cohesive soils: Part I — Method of Analysis. *Comput. Geotech.*, **10**, 87–109, 1990.
- [4] **C.E. Augarde and H.J. Burd**, Three-dimensional finite element analysis of lined tunnels, *Int. J. Num. Meth. Geom.*, **25**, 243–262, 2001.
- [5] **M. Abdel-Meguid**, *Some Three-Dimensional Aspects of Tunneling*, Ph.D. Thesis, University of Western Ontario, 2001 (In preparation).
- [6] **P.T. Brown and J.R. Booker**, Finite element analysis of excavations, *Comput. Geotech.*, **1**(3), 207–220, 1985.
- [7] **G. Gudehus**, Elastoplastische stoffgleichungen für trockenen sand, *Ingenieur-Archiv*, **42**, 1973.

- [8] **H. Matsuoka and T. Nakai**, Stress-deformation and strength characteristics of soil under three different principle stresses, *Proc. JSCE*, **232**, 59–70, 1974.
- [9] **P.V. Lade and J. M. Duncan**, Elasto-plastic stress-strain theory for cohesionless soils, *Proc. ASCE*, **101**, 1037–1053 1975.
- [10] **D.V. Griffiths**, Computation of collapse loads in geomechanics by finite elements. *Ingenieur-Archiv* **59**, 237–244, 1989.
- [11] **O.C. Zienkiewicz and G.N. Pande**, Some useful forms of isotropic yield surfaces for soil and rock mechanics, *Finite Elements in Geomechanics* G. Gudehus, Ed., John Wiley, New York, 1977.
- [12] **T.I. Addenbrooke, D.M. Potts, and A.M. Puzrin**, The influence of pre-failure soil stiffness on the numerical analysis of tunnel construction, *Geotechnique*, **47**(3), 693–712, 1997.
- [13] **O.C. Zienkiewicz and I. C. Cormeau**, Viscoplasticity, plasticity and creep in elastic solids—A unified numerical solution approach, *Int. J. Num. Meth. Eng.*, **8**, 821–845, 1974.
- [14] **GID**, version 6.0. International Centre for Numerical Methods in Engineering. Barcelona, Spain, 1999.
- [15] **R.M.C. Ng and K.Y. Lo**, Measurement of soil parameters relevant to tunneling in clays, *Can. Geotech. J.*, **22**(3), 375–391, 1985.
- [16] **R.K. Rowe and J.R. Booker**, Finite layer analysis of non-homogeneous soils, *ASCE J. Eng. Mech. Div.*, **108**, 115–132, 1982.
- [17] **A.M. Muir Wood**, The circular tunnel in elastic ground, *Geotechnique*, **25**(1), 115–127, 1975.
- [18] **R.K. Rowe, K.Y. Lo, and G.J. Kack**, A method of estimating surface settlement above tunnel constructed in soft ground, *Can. Geotech. J.*, **29**: 11–22, 1983.
- [19] **M. Panet and A. Guenot**, Analysis of convergence behind the face of a tunnel, *Proc. Tunnelling*, Institution of Mining and Metallurgy, London, 197–204.
- [20] **J. Ghaboussi et al.**, Finite element simulations of tunneling over subways, *J. Geotech. Eng. ASCE*, **109**(3), 318–334, 1983.